J|A|C|S
ARTICLES
Published on Web 05/17/2002

Experimental and Theoretical Studies of the Products of Laser-Ablated Thorium Atom Reactions with H_2O in Excess Argon

Binyong Liang,[†] Lester Andrews,*[,†] Jun Li,[‡,§] and Bruce E. Bursten*[,‡]

Contribution from the Department of Chemistry, P. O. Box 400319, University of Virginia, Charlottesville, Virginia 22904-4319, and Department of Chemistry, The Ohio State University, Columbus, Ohio 43210

Received November 26, 2001

Abstract: Reactions of laser-ablated Th atoms with H_2O during condensation in excess argon have formed a variety of intriguing new Th, H, O species. Infrared absorptions at 1406.0 and 842.6 cm^{-1} are assigned to the H−Th and Th═O stretching vibrations of HThO. Absorptions at 1397.2, 1352.4, and 822.8 cm^{-1} are assigned to symmetric H−Th−H, antisymmetric H−Th−H, and Th═O stretching vibrations of the major primary reaction product H_2ThO. Thorium monoxide (ThO) produced in the reaction inserts into H_2O to form HThO(OH), which absorbs at 1341.0, 804.0, and 542.6 cm^{-1}. Both HThO(OH) and ThO_2 add another H_2O molecule to give $HTh(OH)_3$ and $OTh(OH)_2$, respectively. Weaker thorium hydride (ThH_{1-4}) absorptions were also observed. Relativistic DFT and ab initio calculations were performed on all proposed molecules and other possible isomers. The good agreement between experimental and calculated vibrational frequencies, relative absorption intensities, and isotopic shifts provides support for these first identifications of Th, H, O molecular species.

I. Introduction

Actinide chemistry has attracted great attention nowadays because of its relevance to atomic energy, the nuclear industry, and environmental issues. The hydrolysis chemistry of the actinides has a major impact on the design of nuclear waste storage facilities, on nuclear fuel reprocessing cycles, and on nuclear waste remediation processes.[1,2] The aqueous chemistry of thorium has been extensively studied.[3,4] Thorium exists only in the tetravalent state in aqueous solution, and various studies indicate the presence of the hydroxide species $Th(OH)_3^+$, $Th(OH)_2^{2+}$, $Th_2(OH)_2^{6+}$, $Th_4(OH)_8^{8+}$, etc.[5] In addition, the sorption of various cations and anions on hydrous thorium oxide (chemical formula: $ThO_{0.72}(OH)_{2.56}\cdot 3H_2O$) has also been studied.[6] However, little is known about the intermediates and mechanisms of the direct reaction between elemental thorium and water. A systematic experimental and theoretical investigation of the reactivity of Th toward H_2O and the various thorium hydrolysis reaction products should provide greater insight into this chemistry.

Recently, we have characterized a series of small thorium-containing molecules, including ThCO, CThO, NThO, and OThCO, in solid argon or neon by means of laser-ablation and matrix-infrared techniques coupled with density functional theoretical (DFT) calculations.[7−10] These investigations revealed that thorium has surprisingly diverse chemistry and can exist in several oxidation states. Although reactions of beryllium,[11] boron family,[12,13] and transition-metal atoms[14−19] with water have been reported previously using both thermal and laser-ablation methods, the present work is the first comprehensive experimental and theoretical investigations of the reactivities

* To whom correspondence should be addressed. L.A., Tel: (434)924-3513. Fax: (434)924-3710. E-mail: lsa@virginia.edu. B.E.B., Tel: (614)-292-1866. Fax: (614)688-3306. E-mail: bursten.1@osu.edu.
[†] University of Virginia.
[‡] The Ohio State University.
[§] Present address: MS K1-96, 906 Battelle Blvd., Environmental Molecular Sciences Laboratory, Pacific Northwest National Laboratory, Richland, WA 99352.

(1) Engkvist, I.; Albinsson, Y. *Radiochim. Acta* **1992**, *58*/*59*, 109.
(2) Erten, H. N.; Mohammed, A. K.; Choppin G. R. *Radiochim. Acta* **1994**, *66*/*67*, 123.
(3) Ekberg, C.; Albinsson, Y.; Comarmond, M. J.; Brown, P. L. *J. Solution Chem.* **2000**, *29*, 63 and references therein.
(4) Moulin, C.; Amekraz, B.; Hubert, S.; Moulin, V. *Anal. Chim. Acta* **2001**, *441*, 269.
(5) Baes, C. F.; Meyer, N. J.; Roberts, C. E. *Inorg. Chem.* **1965**, *4*, 518.
(6) Mahal, H. S.; Venkataramani, B. *Indian J. Chem., Sect. A* **1998**, *37*, 993 and references therein.
(7) Zhou, M. F.; Andrews, L.; Li, J.; Bursten, B. E. *J. Am. Chem. Soc.* **1999**, *121*, 12188.
(8) Li, J.; Bursten, B. E.; Zhou, M. F.; Andrews, L. *Inorg. Chem.* **2001**, *40*, 5448.
(9) (a) Zhou, M. F.; Andrews, L. *J. Chem. Phys.* **1999**, *111*, 11044. (b) Kushto, G. P.; Andrews, L. *J. Phys. Chem. A* **1999**, *103*, 4836.
(10) Andrews, L.; Zhou, M. F.; Liang, B.; Li, J.; Bursten, B. E. *J. Am. Chem. Soc.* **2000**, *122*, 11440.
(11) Thompson, C. A.; Andrews, L. *J. Phys. Chem.* **1996**, *100*, 12214.
(12) Hauge, R. H.; Kauffman, J. W.; Margrave, J. L. *J. Am. Chem. Soc.* **1980**, *102*, 6005.
(13) Andrews, L.; Burkholder, T. R. *J. Phys. Chem.* **1991**, *95*, 8554.
(14) Kauffman, J. W.; Hauge, R. H.; Margrave, J. L. *J. Phys. Chem.* **1985**, *89*, 3541.
(15) Kauffman, J. W.; Hauge, R. H.; Margrave, J. L. *J. Phys. Chem.* **1985**, *89*, 3547.
(16) Zhang, L. N.; Dong, J.; Zhou, M. F. *J. Phys. Chem. A* **2000**, *104*, 8882.
(17) Zhou, M. F.; Zhang, L. N.; Dong, J.; Qin, Q. Z. *J. Am. Chem. Soc.* **2000**, *122*, 10680.
(18) Zhou, M. F.; Dong, J.; Zhang, L. N.; Qin, Q. Z. *J. Am. Chem. Soc.* **2001**, *123*, 135.
(19) Zhang, L. N.; Zhou, M. F.; Shao, L. M.; Wang, W. N.; Fan, K. N.; Qin, Q. Z. *J. Phys. Chem. A* **2001**, *105*, 6998.

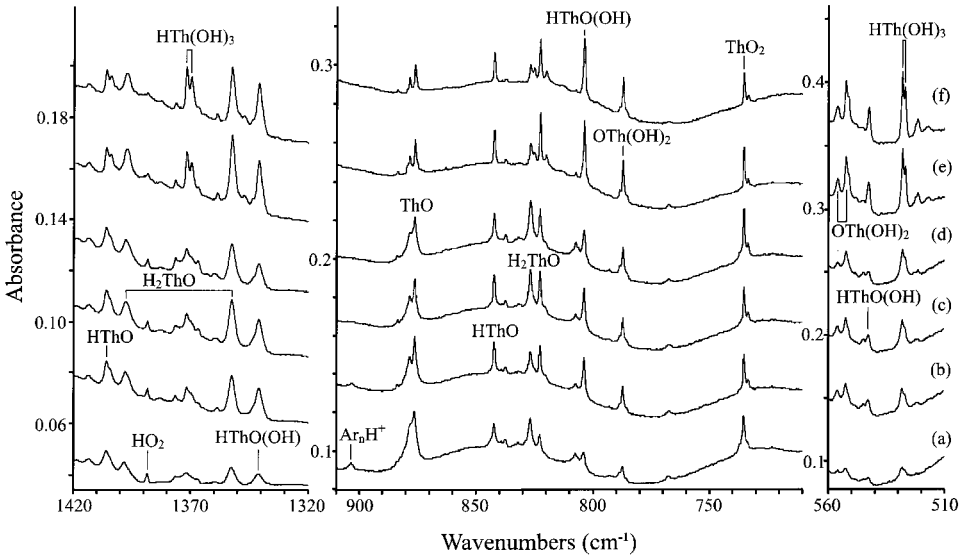

Figure 1. Infrared spectra in the 1420−1320, 910−710, and 560−510 cm^{-1} regions for laser-ablated Th co-deposited with 0.1% H_2O in argon at 7 K. (a) Sample deposited for 80 min, (b) after 25 K annealing, (c) after $\lambda > 380$ nm irradiation, (d) after $\lambda > 240$ nm irradiation, (e) after 35 K annealing, and (f) after 40 K annealing.

and reaction products of an actinide metal atom and water. We will report the matrix infrared spectra that result when laser-ablated thorium atoms react with water molecules. Additionally, relativistic DFT and ab initio calculations have been used to support the spectroscopic assignments and to elucidate the bonding and electronic structures of the novel product molecules. Because a thorium atom has four valence electrons, its chemistry with water molecules might be expected to exhibit similarities to the chemistry of the titanium family of transition elements. As we have seen previously, however, the chemistry of the f-block elements shows distinct differences from that of their d-block analogues.

II. Experimental and Computational Section

The experimental method for laser ablation and matrix isolation has been described in detail previously.[20−22] Briefly, the Nd:YAG laser fundamental (1064 nm, 10 Hz repetition rate with 10 ns pulse width, 3−5 mJ/pulse) was focused onto the rotating thorium metal target (Oak Ridge National Laboratory). Laser-ablated metal atoms were co-deposited with H_2O (0.05−0.5%) in excess argon onto a 7 K CsI cryogenic window at 2−4 mmol/h for 1−1.5 h. Distilled H_2O, D_2O, and $H_2{}^{18}O$ were evaporated from $^1/_4$ in. Swagelok fingers through a Nupro fine metering valve into the argon stream. Additional experiments were also performed for laser-ablated Th atoms reacting with H_2 or D_2 (2%), and O_2 (0.1%) mixtures. Fourier transform infrared (FTIR) spectra were recorded at 0.5 cm^{-1} resolution on a Nicolet 550 spectrometer with 0.1 cm^{-1} accuracy using a mercury−cadmium−telluride (MCTB) detector down to 400 cm^{-1}. Matrix samples were annealed at different temperatures, and selected samples were subjected to irradiation using a medium-pressure mercury lamp ($\lambda > 240$ nm) with the globe removed applying optical filters when needed.

Relativistic DFT calculations were performed using the spin-free Pauli formalism and the Perdew−Wang (PW91) exchange-correlation functional.[23] The frozen core approximation was applied to the [$1s^2$] core of O and the [$1s^2$-$5d^{10}$] core of Th; hence, 12 valence electrons were treated for Th. Slater-type-orbital (STO) basis sets of triple-ζ quality were used for the valence orbitals of Th, H, and O, with d- and f-type polarization functions for the O and p- and d-type polarization functions for the H. The structures of the calculated species were fully optimized with the inclusion of scalar (mass-velocity and Darwin) relativistic effects. Vibrational frequencies were determined via numerical evaluation of the second-order derivatives of the total energies. Throughout the paper, numerical integration accuracy of INTEGRATION = 10.0 and geometry convergence to 10^{-5} were used to accommodate these transient species. All of the calculations were accomplished via the Amsterdam density functional (ADF 2.3) code.[24] Further computational details have been described elsewhere.[25]

Inasmuch as the systems calculated involving metal−hydrogen bonds, we have also carried out ab initio calculations with the second-order Møller−Plesset perturbation theory (MP2) to reinforce the DFT results.[26] The calculations used the Stuttgart energy-consistent quasi-relativistic pseudo-potential and basis set for Th[27] and Pople 6-31G(d) basis sets for H and O.[28] The standard scaling factor (0.9427) is applied to the calculated MP2 frequencies.[29] These calculations were performed using the Gaussian 98 program.[30]

III. Results and Discussion

The products of the reactions of Th atoms with H_2O or with H_2/O_2 mixtures are identified by examination of their infrared spectra with the support of DFT calculations.

A. Th + H_2O. The infrared spectra of the matrix-isolated products from the reaction of thorium atoms and H_2O are shown in Figure 1; the various isotopic substituted spectra are shown in Figures 2−4. The frequencies of the observed bands and their isotopic counterparts are listed in Table 1, along with their

(20) Burkholder, T. R.; Andrews, L. *J. Chem. Phys.* **1991**, *95*, 8697.
(21) Hassanzadeh, P.; Andrews, L. *J. Phys. Chem.* **1992**, *96*, 9177.
(22) Chertihin, G. V.; Saffel, W.; Yustein, J. T.; Andrews, L.; Neurock, M.; Ricca, A.; Bauschlicher, C. W., Jr. *J. Phys. Chem.* **1996**, *100*, 5261.
(23) (a) Perdew, J. P.; Wang, Y. *Phys. Rev. B* **1992**, *45*, 13244. (b) Perdew, J. P.; Chevary, J. A.; Vosko, S. H.; Jackson, K. A.; Peterson, M. R.; Singh, D. J.; Foilhais, C. *Phys. Rev. B* **1992**, *46*, 6671.
(24) ADF 2.3, Theoretical Chemistry, Vrije Universiteit, Amsterdam. (a) Baerends, E. J.; Ellis, D. E.; Ros, P. *Chem. Phys.* **1973**, *2*, 42. (b) te Velde, G.; Baerends, E. J. *J. Comput. Phys.* **1992**, *99*, 94. (c) Fonseca Guerra, C.; Visser, O.; Snijders, J. G.; te Velde, G.; Baerends, E. J. In *Methods and Techniques for Computational Chemistry*; Clementi, E., Corongiu, G., Eds.; STEF: Cagliari, 1995; p 305.
(25) (a) Li, J.; Bursten, B. E. *J. Am. Chem. Soc.* **1997**, *119*, 9021. (b) Li, J.; Bursten, B. E. *J. Am. Chem. Soc.* **1998**, *120*, 11456.
(26) Møller, C.; Plesset, M. S. *Phys. Rev.* **1934**, *46*, 618.
(27) Küchle, W.; Dolg, M.; Stoll, H.; Preuss, H. *J. Chem. Phys.* **1994**, *100*, 7535.
(28) Ditchfield, R.; Hehre, W. J.; Pople, J. A. *J. Chem. Phys.* **1971**, *54*, 724.
(29) Scott, A. P.; Radom, L. *J. Phys. Chem.* **1996**, *100*, 16502.

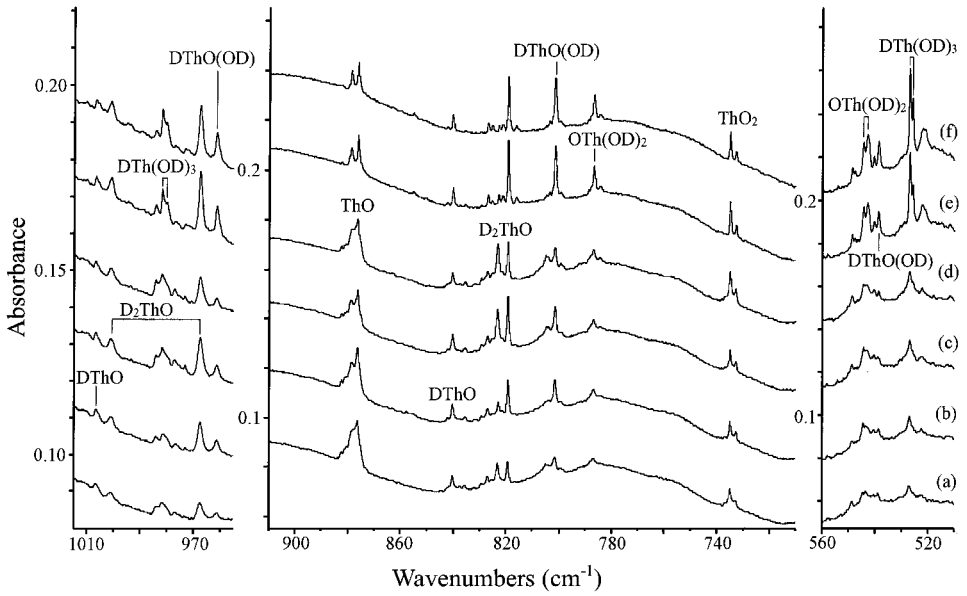

Figure 2. Infrared spectra in the 1015−955, 910−710, and 560−510 cm^{-1} regions for laser-ablated Th co-deposited with 0.1% D_2O in argon at 7 K. (a) Sample deposited for 80 min, (b) after 25 K annealing, (c) after $\lambda > 380$ nm irradiation, (d) after $\lambda > 240$ nm irradiation, (e) after 35 K annealing, and (f) after 40 K annealing.

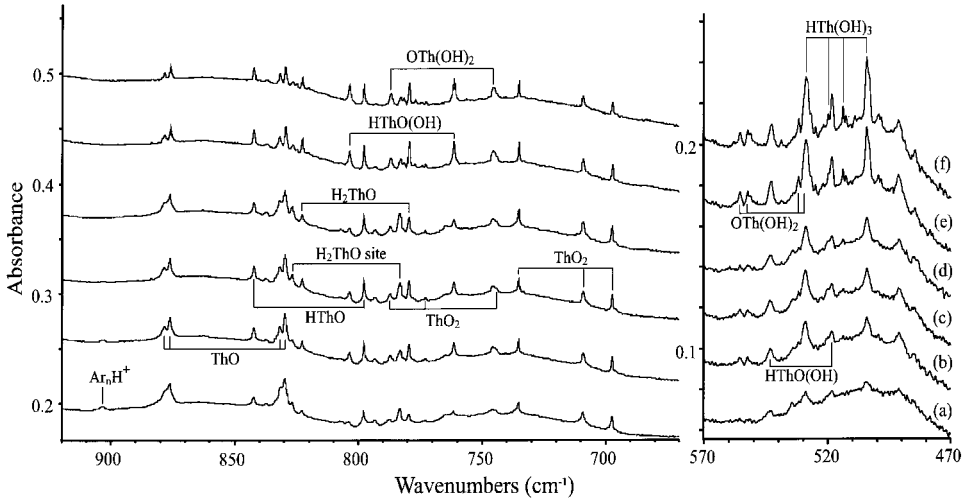

Figure 3. Infrared spectra in the 920−670 and 570−470 cm^{-1} regions for laser-ablated Th co-deposited with 0.1% H_2O + 0.1% $H_2{}^{18}O$ in argon at 7 K. (a) Sample deposited for 80 min, (b) after 25 K annealing, (c) after $\lambda > 380$ nm irradiation, (d) after $\lambda > 240$ nm irradiation, (e) after 35 K annealing, and (f) after 40 K annealing.

proposed assignments. Optimized molecular structures are depicted in Figure 5, and DFT vibrational frequencies of the thorium species identified in this work are given in Table 2. Assignments of the thorium hydrides, ThH (1485.4 cm^{-1}), ThH_2 (1456.0 cm^{-1}), ThH_3 (1435.5, 1434.3 cm^{-1}), ThH_4 (1445.0, 1443.5 cm^{-1}), and oxides, ThO (876.4 cm^{-1}), ThO_2 (787.2, 735.1 cm^{-1}), are inherited from previous work.[9,31,32] In these experiments, the hydride bands showed no ^{18}O isotopic shifts, and not surprisingly, oxide bands showed no deuterium shifts. In a typical experiment, the ThH_{1-4} band intensities are 10−30% of the other products in the 1400 cm^{-1} region. Product bands also included Ar_nH^+ at 903.6 cm^{-1}, Ar_nD^+ at 643.1 cm^{-1},[33] HO_2 and DO_2 at 1388.4 and 1019.8 cm^{-1}.[34] No evidence was found for a Th−OH_2 product in the 1500−1700 cm^{-1} region.

Our DFT calculations of the vibrational frequencies (cm^{-1}) and infrared absorption intensities (km/mol, in parentheses) of the Th hydrides are as follows: ThH_4 (T_d, $^1A_1$), 486(486 × 3), 1430(748 × 3); ThH_3 (C_{3v}, $^2A_1$), 327(78), 576(92 × 2), 1439-(691 × 2), 1494(52); ThH_2 (C_{2v}, $^3B_1$), 530(61), 1424(636), 1479-(240); ThH ($C_{\infty v}$, $^2\Pi$), 1458(143). The quartet $^4\Sigma^-$ ($\sigma^1\delta^2$) ThH

(30) Frisch, M. J.; Trucks, G. W.; Schlegel, H. B.; Scuseria, G. E.; Robb, M. A.; Cheeseman, J. R.; Zakrzewski, V. G.; Montgomery, J. A., Jr.; Stratmann, R. E.; Burant, J. C.; Dapprich, S.; Millam, J. M.; Daniels, A. D.; Kudin, K. N.; Strain, M. C.; Farkas, O.; Tomasi, J.; Barone, V.; Cossi, M.; Cammi, R.; Mennucci, B.; Pomelli, C.; Adamo, C.; Clifford, S.; Ochterski, J.; Petersson, G. A.; Ayala, P. Y.; Cui, Q.; Morokuma, K.; Malick, D. K.; Rabuck, A. D.; Raghavachari, K.; Foresman, J. B.; Cioslowski, J.; Ortiz, J. V.; Stefanov, B. B.; Liu, G.; Liashenko, A.; Piskorz, P.; Komaromi, I.; Gomperts, R.; Martin, R. L.; Fox, D. J.; Keith, T.; Al-Laham, M. A.; Peng, C. Y.; Nanayakkara, A.; Gonzalez, C.; Challacombe, M.; Gill, P. M. W.; Johnson, B. G.; Chen, W.; Wong, M. W.; Andres, J. L.; Head-Gordon, M.; Replogle, E. S.; Pople, J. A. *Gaussian 98*; Gaussian, Inc.: Pittsburgh, PA, 1998.

(31) Souter, P. F.; Kushto, G. P.; Andrews, L.; Neurock, M. *J. Phys. Chem. A* **1997**, *101*, 1287.

(32) Gabelnick, S. D.; Reedy, G. T.; Chasanov, M. G. *J. Chem. Phys.* **1974**, *60*, 1167.

(33) (a) Milligan, D. E.; Jacox, M. E. *J. Mol. Spectrosc.* **1973**, *46*, 460. (b) Wight, C. A.; Ault, B. S.; Andrews, L. *J. Chem. Phys.* **1976**, *65*, 1244.

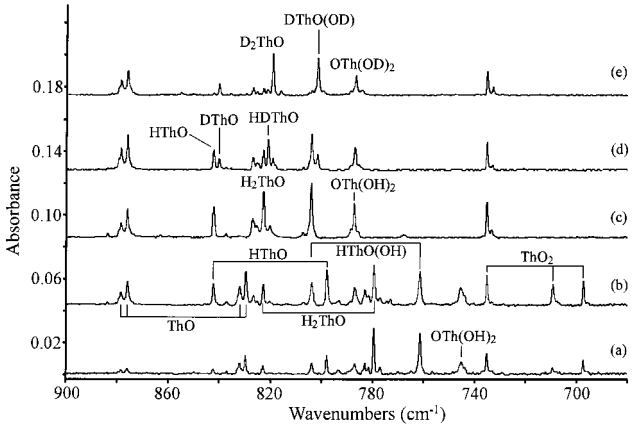

Figure 4. Infrared spectra in the 900−680 cm^{-1} region after 35 K annealing of samples from laser-ablated Th co-deposited with (a) 0.1% $H_2{}^{18}O$, (b) 0.08% H_2O + 0.12% $H_2{}^{18}O$, (c) 0.1% H_2O, (d) 0.15% H_2O + 0.18% HDO + 0.06% D_2O, and (e) 0.1% D_2O in argon at 7 K.

Table 1. Infrared Absorptions (cm^{-1}) of Reaction Products from Laser-Ablated Th Atoms and H_2O in Excess Argon

H_2O	$H_2{}^{18}O$	D_2O	assignment	H_2O	$H_2{}^{18}O$	D_2O	assignment
1485.4	1485.4	1060.3	ThH	878.8	832.0	878.8	ThO site
1456.0	1456.0	1040.6	ThH_2	876.4	829.7	876.4	ThO
1445.0	1445.0		ThH_4	842.6	797.9	840.5	HThO
1443.5	1443.5		ThH_4 site	827.1	783.1	823.3	H_2ThO
1435.5	1435.7		ThH_3	822.8	779.4	819.3	H_2ThO
1434.2	1434.2		ThH_3 site	804.0	761.3	801.6	HThO(OH)
1413.5	1413.4	1010.3	(HTh(OH))	787.2	745.0	786.7	$OTh(OH)_2$
1406.0	1405.9	1006.7	HThO	787.2	744.2		ThO_2 ν_1
1397.2	1396.7	1001.1	H_2ThO	735.1	697.2	735.1	ThO_2 ν_3
1376.5	1376.3	984.2	$HTh(OH)_3$	606.2		595.0	(HTh(OH))
1371.8	1371.5	981.8	$HTh(OH)_3$	556.1	532.0	544.4	$OTh(OH)_2$
1369.9	1369.5	980.1	$HTh(OH)_3$	552.6	529.0	542.9	$OTh(OH)_2$
1352.4	1352.4	967.5	H_2ThO	542.6	518.5	538.8	HThO(OH)
1341.0	1340.8	961.3	HThO(OH)	528.2	504.3	526.9	$HTh(OH)_3$
903.6	903.4	643.1	Ar_nH^+	527.0	503.4	525.8	$HTh(OH)_3$

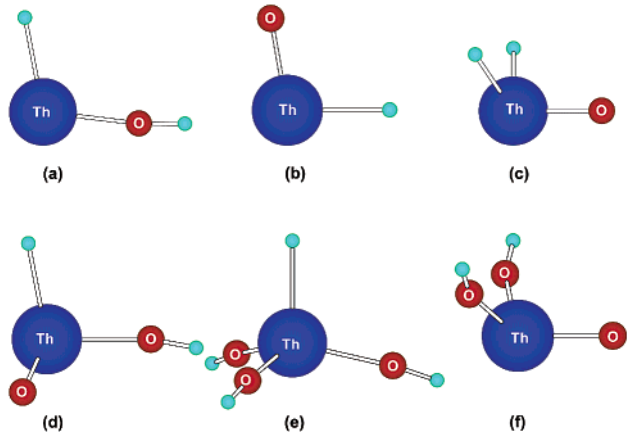

Figure 5. Optimized DFT structures of the thorium-containing species a−f. Bond lengths and angles are given in Table 2.

molecule is only about 1 kcal/mol higher in energy than the $^2\Pi$ ground state. These calculations indicate that the DFT method works well even for Th−H stretching modes. As these ThH_x species have been discussed before,[31] we will not go into the details of the computational results, but only point out that the slightly different frequencies and intensities reported here arise from the much higher integration accuracy used in the present work.

HTh(OH). The primary reaction between Th and H_2O is expected to form the insertion product HTh(OH). Weak bands at 1413.5 and 606.2 cm^{-1} exhibit constant relative intensities and are in the correct range for the Th−H and Th−O vibrations, respectively. In the $H_2{}^{18}O$ experiment, the higher wavenumber band showed very little shift, while the lower band is too weak to be observed. In the D_2O experiment, corresponding bands were observed at 1010.3 and 595.0 cm^{-1}, respectively. In the mixed isotopic experiments, the splitting patterns were not resolved due to the weak nature of both bands. We tentatively assign these two bands to the Th−H and Th−O stretching modes of the HTh(OH) molecule.

Relativistic DFT has been used to characterize more fully the HTh(OH) molecule, which is unusual inasmuch as it is a Th(II) complex. It is interesting to note that even though this molecule may be formed experimentally, we find it to be 32.3 kcal/mol higher than the Th(IV) H_2ThO isomer, which will be discussed later in this paper. The density functional calculations for HTh(OH) predict a planar $^1A'$ ground state with a bent H−Th−O angle close to 108° (Figure 5a). Because this is a Th(II) complex, which has two metal-based electrons, it is somewhat surprising that the ground state is found to be a singlet instead of a triplet. We find that the completely filled HOMO (8a′) of HTh(OH) has 70% Th 7s and 18% Th d_{z^2} character, indicating that the Th 7s orbital is largely unperturbed by the coordination of the ligands. Thus, this Th(II) complex is better described as having an s^2 rather than a d^2 electron configuration at Th. Geometry optimization of the lowest-energy triplet state of the molecule indicates a $^3A''$ state, which corresponds to an s^1d^1 configuration for Th, lying only 3.4 kcal/mol higher in energy.

The Th−H and Th−O vibrational modes are predicted by DFT to occur at 1419 and 656 cm^{-1}, respectively, in nice correspondence to the experimental values. Our calculated $^{16}O/^{18}O$ and H/D isotopic frequency ratios for the two vibrational modes are 1.0525 and 1.0307 for the Th−O mode and 1.0001 and 1.4098 for the Th−H mode.[35] The HTh(OH) molecule is 32.3 kcal/mol higher than the $^1A'$ ground state of the H_2ThO isomer. The corresponding two frequencies calculated by MP2 at 1458 and 652 cm^{-1} (Table 3) become 1374 and 615 cm^{-1} after the standard scaling. Therefore, both DFT and ab initio calculations support observation of the HTh(OH) complex.

HThO. Two bands at 1406.0 and 842.6 cm^{-1} were observed on deposition with integrated intensities of 0.023 and 0.017 au cm^{-1} (au = absorbance units). The higher frequency band is appropriate for a Th−H stretching mode, while the lower is in the correct range for a Th═O stretching mode. These two bands tracked with each other in subsequent annealing and photon-irradiation experiments (Figure 1). Both bands sharpened on annealing to 25 K, did not change upon irradiation, sharpened again on further annealing to 35 K, and finally decreased on annealing to 40 K. In the $H_2{}^{18}O$ experiment, the 1406.0 cm^{-1} band showed a miniscule ^{18}O isotopic shift to 1405.9 cm^{-1}, while the 842.6 cm^{-1} band exhibited a 44.7 cm^{-1} red-shift to 797.9 cm^{-1}, with $^{16}O/^{18}O$ isotopic ratio of 1.0560, which is very close to the 1.0563 ratio observed for diatomic ThO.[9] In the D_2O experiment, the 1406.0 cm^{-1} band red-shifted to 1006.7 cm^{-1}, and the 842.6 cm^{-1} band shifted

(34) (a) Milligan, D. E.; Jacox, M. E. *J. Chem. Phys.* **1963**, *38*, 2627. (b) Smith, D. W.; Andrews, L. *J. Chem. Phys.* **1974**, *60*, 81.

Table 2. Ground Electronic States, Equilibrium Geometries, and Isotopic Frequencies Calculated for Possible Th + H_2O Reaction Products[a]

species	elec state, point group	geometry (Å, deg)		frequencies, cm^{-1} (intensities, km/mol)
HThO	$^2A'$, C_s	Th−H: 2.054, Th═O: 1.869, ∠HThO: 100.2	H-^{16}O	337(78), 848(209), 1417(346)
			D-^{16}O	270, 845, 1007
			H-^{18}O	365, 803, 1417
HTh(OH)	$^1A'$, C_s	Th−O: 2.028, Th−H: 2.033, O−H: 0.964, ∠HThO: 107.6, ∠ThOH: 173.6	H-^{16}O	153(43), 472(93), 483(80), 656(70), 1419(252), 3851(356)
			D-^{16}O	113, 348, 361, 636, 1007, 2811
			H-^{18}O	153, 470, 479, 623, 1419, 3837
H_2ThO	$^1A'$, C_s	Th−H: 2.078, Th═O: 1.876, ∠OThH: 100.8, ∠HThH: 103.6	H-^{16}O	356(159), 388(0), 464(94), 837(220), 1373(646), 1426(310)
			D-^{16}O	260, 288, 329, 833, 974, 1015
			H-^{18}O	354, 386, 464, 793, 1373, 1426
HThO′(OH)	^1A, C_1	Th−H: 2.108, Th═O′: 1.894, Th−O: 2.109, O−H: 0.964; ∠HThO′: 102.1, ∠HThO: 101.4, ∠OThO′: 107.5, ∠ThOH: 160.5	H-^{16}O	146(17), 300(123), 375(91), 406(145), 456(141), 600(198), 817(206), 1359(436), 3834(147)
			D-^{16}O	139, 219, 274, 313, 344, 578, 815, 967, 2795
			H-^{18}O	139, 298, 373, 402, 452, 572, 774, 1359, 3821
O′Th$(OH)_2$	$^1A'$, C_s	Th═O′: 1.910, Th−O: 2.140, O−H: 0.964, ∠O′ThO: 106.2, ∠OThO: 112.2, ∠ThOH: 161.4	H-^{16}O	92(6), 126(9), 163(16), 350(7), 373(270), 429(144), 458(207), 555(209), 585(100), 801(185), 3833(149), 3834(65)
			D-^{16}O	86, 120, 154, 273, 284, 323, 350, 536, 567, 800, 2794, 2794
			H-^{18}O	88, 120, 155, 346, 370, 425, 454, 530, 556, 758, 3820, 3821
$H_2Th(OH)_2$	$^1A_1$, C_{2v}	Th−H: 2.104, Th−O: 2.100, O−H: 0.964, ∠HThH: 108.3, ∠HThO: 106.4, ∠OThO: 122.5, ∠ThOH: 173.9	H-^{16}O	84(3), 204(89), 347(0), 350(227), 425(241), 433(0), 437(104), 461(155), 492(136), 602(376), 623(164), 1359(754), 1403(397), 3841(235), 3842(112)
$HTh(OH)_3$	$^1A_1$, C_{3v}	Th−H: 2.117, Th−O: 2.117, O−H: 0.964, ∠HThO: 103.6, ∠ThOH: 174.7	H-^{16}O	94(0), 101(4 × 2), 362(116 × 2), 399(0), 437(181 × 2), 452(320), 456(39 × 2), 580(330 × 2), 622(40), 1364(503), 3842(196 × 2), 3845(52)
			D-^{16}O	88, 95, 263, 298, 327, 339, 343, 561, 603, 968, 2801, 2805
			H-^{18}O	90, 96, 360, 397, 434, 448, 453, 553, 589, 1364, 3828, 3831

[a] ADF.

Table 3. Unscaled MP2 Vibrational Frequencies and Infrared Intensities (in parentheses) of the Thorium−Water Reaction Products[a]

species						
HThO	388(83)	839(158)	1452(363)			
HTh(OH)	262(21)	450(137)	461(99)	652(83)	1458(380)	3786(289)
H_2ThO	362(175)	410(0.2)	488(110)	826(163)	1442(656)	1471(330)
HThO(OH)	141(29)	304(144)	385(106)	415(125)	442(194)	608(183)
	806(163)	1427(452)	3805(190)			
$OTh(OH)_2$	113(18)	127(6)	153(11)	320(16)	346(332)	428(201)
	459(183)	565(181)	595(122)	788(154)	3818(189)	3819(120)
$H_2Th(OH)_2$	105(2)	222(35)	326(73)	326(0)	337(365)	366(278)
	387(185)	398(0)	506(148)	619(373)	642(204)	1417(772)
	1450(375)	3822(296)	3823(168)			
$HTh(OH)_3$	104(0)	115(3 × 2)	289(0)	342(307 × 2)	371(24 × 2)	383(445)
	393(474 × 2)	594(643 × 2)	633(62)	1425(514)	3829(507 × 2)	3830(66)

[a] Gaussian 98.

only to 840.5 cm^{-1}. In the mixed H_2O + HDO + D_2O experiment (Figure 4d), the lower band clearly showed a doublet feature at 842.6 and 840.5 cm^{-1}, while both the 1406.0 and the 1006.7 cm^{-1} bands were identified even though strong HDO absorptions dominated the spectral region around 1400 cm^{-1}. In the mixed $H_2{}^{16}O$ + $H_2{}^{18}O$ isotopic experiments (Figure 3), a doublet was observed for the lower band at 842.6 and 797.9 cm^{-1}. Both mixed isotopic experiments clearly indicated that single H and O atoms are involved in the responsible molecule. Therefore, these two bands are assigned to the Th−H and Th═O stretching vibrations in the HThO molecule, respectively.

Our density functional calculations predict a $^2A'$ ground electronic state for the HThO molecule, with Th−H and Th═O bond lengths of 2.054 and 1.869 Å, and ∠HThO = 100.2° (Table 2 and Figure 5b). The vibrational analyses predicted Th−H and Th−O stretching modes at 1417 and 848 cm^{-1}, with absorption intensities of 346 and 209 km/mol, respectively. Both of the vibrational frequencies agree extremely well (within 1%) with the experimental values. The predicted intensities and calculated isotopic ratios (Table 2) are in similar good agreement with the experimental observations. Another isomer of HThO, the Th(I) molecule ThOH, was also calculated. We find a linear $^2\Delta$ ($\sigma^2\delta^1$) ground state for ThOH with vibrational frequencies at 499, 652, and 3850 cm^{-1}. However, this linear isomer is 37.1 kcal/mol higher in energy than HThO, and ThOH is not observed experimentally. Ab initio MP2 calculation predicts the frequencies of HThO at 388, 839, 1452

cm^{-1} or scaled frequencies at 366, 791, and 1369 cm^{-1}, which are in slightly poorer agreement than the DFT results.

H_2ThO. The 822.8 cm^{-1} band observed after deposition, doubled on 25 K annealing, increased a little on $\lambda > 380$ nm irradiation, then decreased upon full-arc Hg-lamp irradiation. The band increased again on 35 K annealing, and finally decreased on 40 K annealing. This band, which is in the Th═O stretching region, red-shifted to 779.4 cm^{-1} in the $H_2{}^{18}O$ experiment. The $^{16}O/^{18}O$ isotopic ratio of 1.0557 nearly matches the value of 1.0563 for diatomic ThO. In the mixed $H_2{}^{16}O + H_2{}^{18}O$ experiment, only a doublet with two pure isotopic bands was observed. In the D_2O experiment, this band showed a small but definite red-shift to 819.3 cm^{-1}. It seems evident that this band is due to a H-perturbed Th═O vibration. More decisive data are obtained from the mixed $H_2O + HDO + D_2O$ (molar ratio of H:D is about 1.6:1) experiment; the band splits and clearly shows a triplet feature with a new 821.1 cm^{-1} band in the middle of two pure isotopic bands (Figure 4d). This band is assigned as a Th═O vibrational mode perturbed by two equivalent hydrogen atoms.

In the Th−H vibrational region near 1400 cm^{-1}, bands at 1397.2 and 1352.4 cm^{-1} tracked with the 822.8 cm^{-1} band throughout all experiments. After 35 K annealing (when the three bands have their strongest absorptions), the integrated intensities of these bands (1397.2, 1352.4, and 822.8 cm^{-1}) are 0.039, 0.079, and 0.032 au cm^{-1}, respectively. The 1397.2 cm^{-1} band red-shifted to 1001.1 cm^{-1} in the D_2O experiment, and to 1396.7 cm^{-1} in the $H_2{}^{18}O$ experiment. The 1352.4 cm^{-1} band red-shifted to 967.5 cm^{-1} with D_2O, but no ^{18}O shift was observed. The 1397.2 and 1352.4 cm^{-1} bands are assigned as the symmetric and antisymmetric stretching vibrations in a symmetrical H−Th−H unit, respectively. These assignments are also well-supported by the mixed $H_2O + HDO + D_2O$ experiment, where two new bands at 1375.1 and 983.7 cm^{-1} tracked with the aforementioned three bands. The 1375.1 cm^{-1} band is only 0.3 cm^{-1} higher than the median of the 1397.2 and 1352.4 cm^{-1} bands, and 983.7 cm^{-1} is only 0.6 cm^{-1} lower than the median of the 1001.1 and 967.5 cm^{-1} bands, which are the deuterium counterparts of the 1397.2 and 1352.4 cm^{-1} bands. These two new bands are assigned to the Th−H and Th−D stretching vibrations in a H−Th−D unit where nearly no interaction occurs between two modes because of the large mass of thorium and difference between H and D atoms. All of these data point to formation of the previously unknown Th(IV) molecule H_2ThO.

The H_2ThO molecule is potentially very important. First, it is a Th(IV) complex, which indicates that it might be a ubiquitous species in the chemistry of Th with H_2O. Second, it increases in annealing experiments, which suggests its spontaneous formation in the reaction between Th and H_2O. Third, this molecule is analogous to the recently reported H_2MO (M = Ti, Zr, Hf) molecules.[17] Our relativistic DFT calculation predicts a C_s geometry for H_2ThO, corresponding to a pyramidal structure, with a $^1A'$ ground state. The calculated geometry has Th═O = 1.876 Å, Th−H = 2.078 Å, ∠HThH = 103.6°, and ∠OThH = 100.8° (Figure 5c). The vibrational analysis predicts three modes at 1426, 1372, and 837 cm^{-1} with infrared intensities of 310, 646, and 220 km/mol, respectively. These results correspond to the experimental values very well, the frequencies are higher by 2.1, 1.4, and 1.7%, respectively, and the relative intensities are also well matched. A planar form of H_2ThO (C_{2v},$^1A_1$) lies 6.1 kcal/mol higher in energy than the pyramidal geometry; an imaginary frequency (357*i* cm^{-1}) for the C_{2v} structure confirms that this is a transition state between two C_s geometries. Triplet C_s and C_{2v} structures are found to be at least 54.5 kcal/mol higher than the $^1A'$ ground state. The calculated MP2 frequencies are 826, 1442, and 1471 cm^{-1}, which become 779, 1359, and 1387 cm^{-1} after scaling. These frequencies are also very close to the experimental values further supporting the above assignments.

The 827.1 cm^{-1} band is most likely due to a matrix splitting of the 822.8 cm^{-1} absorption for H_2ThO, possibly owing to different reaction mechanisms. This 827.1 cm^{-1} band has isotopic shifts and mixed isotopic splitting patterns similar to the 822.8 cm^{-1} band. However, it increased on irradiation, but decreased on annealing. These observations indicate that H_2ThO could be formed via the photoinduced reaction between a thorium atom and a water molecule. The initial 827.1 cm^{-1} absorption observed after deposition is likely due to the same mechanism where the laser plume serves as a photolysis source.

HThO(OH). The band at 804.0 cm^{-1} was weaker on deposition as compared to the HThO absorption at 842.5 cm^{-1}, but it almost tripled in intensity upon 25 K annealing. The band decreased by one-third on full-arc irradiation, then doubled upon 35 K annealing. This band has a signature ^{18}O red-shift to 761.3 cm^{-1}, with $^{16}O/^{18}O$ isotopic ratio of 1.0561. With D_2O the band red-shifted to 801.6 cm^{-1}. In both mixed isotopic experiments ($^{16}O/^{18}O$ and H/D), only doublets were observed. This absorption is an appropriate frequency for a Th═O vibrational mode, but H is slightly involved. The 1341.0 cm^{-1} band was also observed on deposition, and tracked with the 804.0 cm^{-1} band throughout the annealing and irradiation cycles. This band showed a very small 0.2 cm^{-1} ^{18}O shift, and red-shifted to 961.3 cm^{-1} with D_2O, which characterizes a Th−H vibration with very little oxygen participation. A third band at 542.9 cm^{-1} tracked with the 804.0 and 1340.8 cm^{-1} bands, and red-shifted to 518.5 cm^{-1} in the $H_2{}^{18}O$ experiment, and to 538.8 cm^{-1} in the D_2O experiment. This band position is appropriate for a Th−O dominated vibration. The $^{16}O/^{18}O$ isotopic ratio of 1.0465 is smaller than that of diatomic ThO, 1.0563, while the H/D ratio of 1.0071 is larger than that found for the Th═O modes in both the HThO and the H_2ThO molecules. This larger H/D ratio suggests that the perturbing H-atom bonds to the lighter atom of the Th−O vibrator; that is, it implies the presence of a Th−OH group. We therefore propose that these three bands are due to the HThO(OH) molecule. Another signature infrared mode in this molecule would be the O−H stretch, but very strong H_2O bands dominated the spectral region around 3800 cm^{-1}, and we cannot definitively identify this mode. Finally, the relative intensities of these three bands (1341.0, 804.0, and 542.6 cm^{-1}) are about 6:4:3 (after 35 K annealing, the integrated intensities are 0.067, 0.043, 0.033 au cm^{-1}, respectively).

Like H_2ThO, HThO(OH) is a Th(IV) complex that is expected to have a closed-shell singlet ground state. The DFT calculation on HThO(OH) was first performed under C_s symmetry with the molecule restricted to being planar. This geometrical constraint led to an imaginary frequency for the out-of-plane H−Th bond bending mode, indicating that a nonplanar structure is lower in energy. When the geometrical constraint of planarity

was relaxed, the molecule converged to a pyramidal structure (C_1 symmetry) with a closed-shell ^{1}A ground state that is 5.1 kcal/mol lower in energy than the planar geometry. In this pyramidal geometry, the Th−H bond forms a 110.1° angle with the OThO plane (Figure 5d). Other geometric parameters are listed in Table 2.

The DFT vibrational analysis predicts three modes at 1359 (Th−H), 817 (Th═O), and 599 (Th−OH) cm^{-1} with absorption intensities of 436, 206, and 198 km/mol (6.6:3.1:3). The two higher frequency modes agree well with the experimental values, differing by only 1.3 and 1.6%, respectively. The good agreement between the isotopic frequencies, which indicates that both modes are well-described by the calculation, is also worth noting. The calculated Th−OH stretching frequency is about 57 cm^{-1} too high, and this mode is also calculated to be highly mixed; the calculations predict that the hydrogen atom of the hydroxyl group is highly involved in this vibrational mode. However, the small experimental deuterium shift indicates much less hydrogen involvement than is predicted from the calculations.

Given the large discrepancy between the calculated and observed Th−OH stretching frequency, it is interesting to compare the DFT results to those from an MP2 calculation to test the sensitivity of the frequency to the method used. The MP2 frequencies for HThO(OH) are 1427, 806, and 608 cm^{-1}, which with scaling become 1345, 760, and 573 cm^{-1}, with intensity ratio 7.4:2.7:3. Here the scaled frequency of 573 cm^{-1} is still about 30 cm^{-1} too high, suggesting that this mode might be influenced by the matrix environment. Metal−oxygen stretching modes are indeed expected to exhibit larger matrix effects.

HTh(OH)$_3$. A broad band at 1371.7 cm^{-1} was also observed on deposition. This band increased and sharpened after 25 K annealing, increased slightly upon $\lambda > 380$ nm irradiation, and did not change on full-arc irradiation. The band markedly increased on 35 K annealing, and still increased on 40 K annealing, while all absorptions due to the aforementioned molecules decreased. This annealing behavior suggests that this absorption may be due to a molecule formed in secondary reactions of the initial product with excess H_2O in the matrix. In the $H_2{}^{18}O$ experiment, only a 0.3 cm^{-1} ^{18}O red-shift was observed. The deuterium isotopic counterpart of this band was observed at 981.8 cm^{-1}, which confirms it as a Th−H vibrational mode. A related absorption was observed at 528.2 cm^{-1} and has ^{18}O and D counterparts at 504.3 and 526.9 cm^{-1}. In the mixed $H_2{}^{16}O + H_2{}^{18}O$ experiment, this band shows a 4:1:1:4 quartet feature with two new intermediate bands at 519.9 and 513.9 cm^{-1}. This isotopic splitting pattern is characteristic of the doubly degenerate mode of a trigonal species.[35] In the mixed H/D experiment, unfortunately, the small deuterium shift allowed only a broad band centered at 527 cm^{-1} to be observed, and no isotopic splitting pattern could be resolved. These two bands at 1371.8 and 528.2 cm^{-1} are proposed for the Th−H stretching mode and the doubly degenerate Th−O stretching mode in a C_{3v} HTh(OH)$_3$ molecule, respectively.

The DFT calculation for a singlet HTh(OH)$_3$ molecule with C_{3v} symmetry predicts three strong absorptions at 3841, 1364, and 580 cm^{-1}. While the doubly degenerate O−H stretching mode is obscured by the strong H_2O absorptions around 3800 cm^{-1}, the other two modes differ by 0.6 and 9.8%, respectively. Again, the calculations indicate strong mixing between the Th−O and Th−H stretching modes. The MP2 calculations performed on this molecule produce 3829, 1425, and 594 cm^{-1}, which become 3610, 1343, and 560 cm^{-1} after scaling. Once again, the scaled MP2 frequency at 560 cm^{-1} is about 32 cm^{-1} too high.

OTh(OH)$_2$. The band at 787.2 cm^{-1} on deposition is the symmetric stretching mode (ν_1) of the ThO_2 molecule.[32] However, this band did not track with the antisymmetric stretching mode (ν_3, at 735.1 cm^{-1}) of the same ThO_2 molecule on annealing. The band became broader in the D_2O experiment, but no obvious band splitting was observed. In the $H_2{}^{18}O$ experiment, the band does split with a major peak at 745.7 and a shoulder at 744.2 cm^{-1}. On the basis of previous work[32] and new Th + O_2 results in this laboratory for the relative absorption intensities of ν_1 and ν_3 modes of ThO_2, we believe the 787.2 cm^{-1} band represents absorption due to another molecule in addition to ThO_2. The shoulder at 744.2 cm^{-1} observed in the $H_2{}^{18}O$ experiment is the ν_1 mode of $Th^{18}O_2$, and a new band at 772.7 cm^{-1} observed in the $H_2{}^{16}O + H_2{}^{18}O$ experiment is the ν_1 mode of $Th^{16}O^{18}O$. What is the other species responsible for the absorption at 787.2 cm^{-1}? This band is in the Th═O vibrational region, and has a ^{16}O/^{18}O ratio of 1.0557. It showed a doublet in the $H_2{}^{16}O + H_2{}^{18}O$ experiment, and has a very small deuterium shift. The absorber should have a Th═O bond with some other hydrogen-containing ligands bonded to the thorium atom.

Bands at 556.1 and 552.6 cm^{-1} apparently track with the unknown 787.2 cm^{-1} band, although the complication of the latter makes this observation less definitive. The 552.6 cm^{-1} band shifts to 529.0 and 542.9 cm^{-1} in $H_2{}^{18}O$ and D_2O experiments, respectively. The isotopic ^{18}O and D shifts are appropriate for a Th−O vibrational mode in a Th−OH unit. No intermediate band was observed in the $H_2{}^{16}O + H_2{}^{18}O$ experiment, but such a band could possibly be covered by the HThO(OH) absorption at 542.6 cm^{-1}. In the mixed H/D experiment, a 1/2/1 triplet with an intermediate band at 548.6 cm^{-1} was observed, which reveals that there are two equivalent Th−OH units involved. We tentatively assign the 787.2 and 552.6 cm^{-1} bands to the Th═O and antisymmetric Th−O stretching mode of an OTh(OH)$_2$ molecule. In light of the recently reported $H_2M(OH)_2$ (M = Ti, Zr, Hf) molecules,[17] it also seems possible that the 552.6 cm^{-1} band might be due to $H_2Th(OH)_2$. However, our DFT calculations favor the assignment as OTh(OH)$_2$ rather than $H_2Th(OH)_2$ as based on the calculated vibrational frequencies.

The DFT calculation of OTh(OH)$_2$ was performed on a planar C_{2v} structure first, but, as for some of the other molecules, this geometry led to an imaginary vibrational frequency. A nonplanar OTh(OH)$_2$ with C_s symmetry (Figure 5f) was found to be 6.0 kcal/mol lower in energy than the C_{2v} structure. The Th−OH bond lengths in the nonplanar structure are 0.03 Å shorter than those in the planar structure, indicating stronger bonding in the lower symmetry. The Th═O and antisymmetric Th−OH modes are predicted to occur at 801 and 585 cm^{-1}, which agree well with experimental data. Interestingly, despite the difference between oxo and hydroxyl groups, the calculated geometry of OTh(OH)$_2$ (C_s symmetry) can be described as having pseudo-C_{3v} symmetry, as shown by the near-degenerate vibrational

(35) Darling, J. H.; Ogden, J. S. *J. Chem. Soc., Dalton Trans.* **1972**, 2496.

frequencies of some of the modes. The calculation on $H_2Th(OH)_2$ predicted a C_{2v} structure with a $^1A_1$ ground state, antisymmetric Th−OH mode at 602 cm^{-1}, and two very strong infrared absorptions near 1400 cm^{-1}, which are not observed experimentally. Our MP2 calculations give similar results (Table 3).

B. Th + H_2/O_2. Reactions were also done between Th atoms and H_2/O_2 mixtures using similar laser power and gas flow rates. The product bands include strong ThO_2 absorptions (both ν_1 and ν_3, with relative intensities of 1:4), a relatively weaker ThO absorption (about one-eighth the intensity of the ThO_2 ν_3 mode), strong ThH_2, ThH_3, ThH_4 bands, and a relatively weaker ThH band (about one-sixth the intensity of the ThH_2 absorption).[31,32] Bands for HO_2 and Ar_nH^+ are also observed.[33,34] Reaction products involving both oxygen and hydrogen atoms include HThO at 842.7 cm^{-1}, and HThO(OH) bands at 1341.0, 804.0, and 542.6 cm^{-1}. After 35 K annealing, $HTh(OH)_3$ is observed. Another experiment was done with a D_2/O_2 mixture, and the same deuterium isotopic shifts were observed for the HThO, HThO(OH), and $HTh(OH)_3$ bands as in the Th + D_2O experiment. The markedly reduced yield of H_2ThO in the H_2/O_2 investigations is noteworthy. This seems to indicate that H_2ThO is not readily formed from the elements, nor from the reaction of H_2 with ThO, but is formed by rearrangement of the primary product of the reaction between Th and H_2O.

IV. Electronic Structure and Bonding in New Thorium Complexes

The reactions between Th atoms and H_2O molecules produce several new molecules that challenge some of our notions of structure and bonding in actinide chemistry. In this section, we will focus on the electronic structure of two of the more interesting new species that result from the 1:1 reaction of Th and H_2O, the Th(II) complex HTh(OH) and the Th(IV) complex H_2ThO.

Th(II) Complexes. One of the interesting aspects of this work is the apparent production of several fundamental new molecules of Th, including the Th(II) complex HTh(OH) in addition to ThH_2 and the monoxide ThO. The HTh(OH) molecule is fascinating for several reasons: (1) It appears to be the primary product of the reaction between a Th atom and an H_2O molecule, (2) it is a simple example of a complex of Th(II), which is a highly unusual oxidation state of Th, and (3) it is predicted to have a singlet ground state and a bent geometry, both of which are not intuitive. To address some of these matters, we have delved more deeply into the electronic structure of and bonding in some simple Th(II) complexes. We will see that the results are consistent with the position Th has as a very electropositive element with high-lying 5f orbitals relative to later actinide elements.

The ground electron configuration of a Th atom is $[Rn]7s^2-6d^2$. A Th(II) complex could, in principle, retain its two metal-based electrons in an s^2, an s^1d^1, or a d^2 configuration, or could use the higher-lying vacant 5f orbitals. The relative energies of the 7s, 6d, and 5f orbitals in a Th complex will be sensitive to the ligands present. For example, the ligand field provided by three substituted cyclopentadienyl ligands causes the organothorium(III) complexes Cp_3Th (Cp = cyclopentadienyl or substituted cyclopentadienyl) to have a d^1 configuration.[36] A recently characterized Th(III) sandwich complex, $[Th(COT')_2]^-$ (COT′ = η^8-1,4-(*t*-$BuMe_2Si)_2C_8H_6$), also has a d^1 configuration.[37] In both of these cases, the ligand field is strong enough and isotropic enough to destabilize the 7s orbital well above the 6d orbitals, and the 5f orbitals are too high in energy to be used to house the metal-based electron.

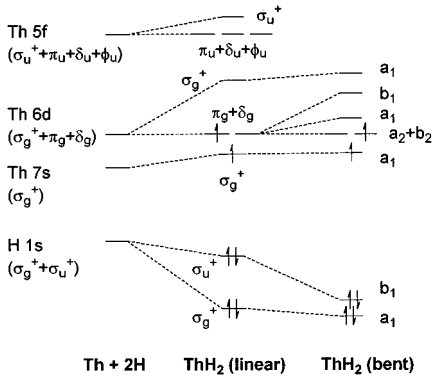

Figure 6. Qualitative molecular orbital energy level diagrams of linear and bent ThH_2. The leftmost columns show the formation of the MOs of linear ThH_2 from the AOs of Th and 2H, while the right column shows the energy levels of bent ThH_2. The Th 5f-based MOs for bent ThH_2 are not relevant to the discussion and are omitted for clarity.

Before addressing the bonding in HTh(OH), we find it helpful to examine the even simpler Th(II) hydride, ThH_2, in both linear ($D_{\infty h}$) and bent (C_{2v}) geometries. Construction of a molecular orbital diagram for linear ThH_2 under the $D_{\infty h}$ single group (i.e., with no spin−orbit coupling) is very straightforward. The H 1s orbitals are lower in energy than the Th orbitals, which follow the order 7s < 6d < 5f. Interaction of the H 1s AOs with the Th orbitals leads to the formation of symmetric (σ_g) and antisymmetric (σ_u) Th−H bonding MOs that are predominantly H 1s in character. The symmetric MO can involve contributions from the Th 7s and $6d_{z^2}$ AOs, whereas the antisymmetric MO can involve the Th $5f_{z^3}$ and $7p_z$ AOs.

Our relativistic calculations on linear ThH_2 indicate that the σ_g MO has AO contributions of 59% H 1s, 15% Th 7s, and 26% $6d_{z^2}$. The σ_u MO has contributions of 72% H 1s, 20% Th $5f_{z^3}$, and 6% Th $7p_z$. Notice that this MO involves smaller contributions from the Th atom, which results from the high energies of the Th $5f_{z^3}$ and $7p_z$ AOs. By symmetry, the Th 6dπ (d_{xz}, d_{yz}) and 6dδ ($d_{x^2-y^2}$, d_{xy}) AOs cannot interact with the H 1s orbitals, and they remain as nonbonding orbitals. The energy levels of linear ThH_2 under this simple bonding scheme are shown in Figure 6. Because the 6dπ and 6dδ AOs are still low in energy, we find that linear ThH_2 has a triplet ground state corresponding to an s^1d^1 configuration.

In linear ThH_2, the antisymmetric combination of the H 1s orbitals can only interact with the f and p orbitals of the Th atom. For actinide atoms, in general, and for Th, in particular, it is advantageous to use the 6d orbitals as the preferential acceptor orbitals for ligand donation.[38] By reducing the symmetry via bending of the molecule, the antisymmetric combination of the H 1s orbitals is allowed to interact with a Th 6d orbital:

(36) (a) Kot, W. K.; Shalimoff, G. V.; Edelstein, N. M.; Edelman, M. A.; Lappert, M. F. *J. Am. Chem. Soc.* **1988**, *110*, 986. (b) Bursten, B. E.; Rhodes, L. F.; Strittmatter, R. J. *J. Am. Chem. Soc.* **1989**, *111*, 2756.
(37) Parry, J. S.; Cloke, F. G. N.; Coles, S. J.; Hursthouse, M. B. *J. Am. Chem. Soc.* **1999**, *121*, 6867.
(38) Bursten, B. E.; Strittmatter, R. J. *Angew. Chem., Int. Ed. Engl.* **1991**, *30*, 1069.

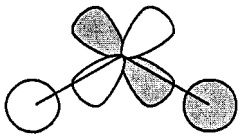

Our DFT calculations indicate that allowing ThH_2 to bend gains 16 kcal/mol in energy. The converged molecule has $\angle H-Th-H = 114.2°$. The significant bending of the molecule allows the interaction sketched above to occur quite readily, as is evident from the characters of the antisymmetric Th−H bonding MO: 59% H 1s, 35% Th 6d, and 2% Th 5f. In essence, by bending, the Th atom has shifted the responsibility of charge acceptance in the antisymmetric orbital from the 5f to the 6d orbitals. The strength of this interaction is such that the optimized Th−H bond length in bent ThH_2 (2.033 Å) is 0.084 Å shorter than that in linear ThH_2 (2.117 Å).

The symmetric Th−H bonding MO in bent ThH_2 uses both the Th 7s and the 6d orbitals as acceptor orbitals. We find that the AO contributions to this orbital are 61% H 1s, 21% Th 7s, and 12% Th 6d. Even after bending, two of the Th 6d orbitals are still unable to interact with the H 1s orbitals by symmetry. As a consequence, the energy gap between the Th 7s orbital and the nonbonding Th 6d orbitals is small enough (ca. 0.6 eV) that bent ThH_2 still prefers to have a triplet ground state with an s^1d^1 configuration at the Th(II) center. The changes in the MO energies of ThH_2 upon bending are shown in Figure 6. ThH_2 has been observed and characterized as a bent molecule with symmetric and antisymmetric stretching modes observed at 1480 and 1456 cm^{-1}.[31]

Like ThH_2, HTh(OH) is predicted to be a bent molecule with $\angle H-Th-O = 120.8°$. The HTh(OH) molecule is bent for the same reason that ThH_2 is, to facilitate greater donation from the H and OH ligands into the Th 6d orbitals. There are differences between HTh(OH) and ThH_2, however, most notably our prediction that HTh(OH) should be a closed-shell singlet molecule. The source of this difference in the ground state is the presence of the p lone pairs on the O atom. The Th−O−H linkage is close to linear, with $\angle Th-O-H = 168.5°$. Thus, both of the π lone pairs on the O atom will be appropriately disposed to interact with empty orbitals on the Th atom. Of particular importance is the donation from the out-of-plane O π lone pair into one of the previously nonbonding Th 6d orbitals:

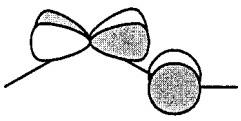

The π donation from the O atom to the Th atom, coupled with the more directed O s donation (relative to that of the H atom), leads to a strong bond between Th and O. As a result, the Th−O bond length in HTh(OH) (2.038 Å) is nearly identical to the Th−H bond length (2.030 Å).

The destabilization of the Th 6d orbitals by donation from the O π lone pairs increases the gap between the MO that is predominantly Th 7s in character and the lowest one that is Th 6d-based from ca. 0.6 eV in bent ThH_2 to ca. 0.85 eV in HTh(OH). That slight increase is enough to favor spin-pairing to an s^2 configuration at Th and a singlet ground state. As noted earlier, the open-shell s^1d^1 triplet state lies only 3.4 kcal/mol above the ground state.

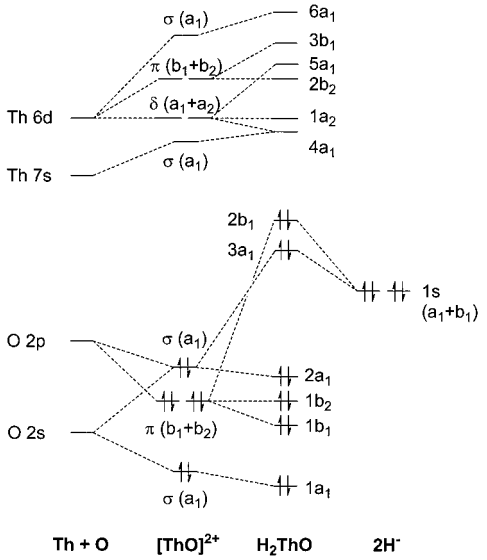

Figure 7. Molecular orbital interaction diagram, based on the relativistic DFT calculations for planar H_2ThO in which the molecule is constructed from the interaction of the 1s atomic orbitals of two H^- ions with the frontier orbitals of a $[ThO]^{2+}$ fragment.

H_2ThO. The most stable isomer of Th + H_2O, H_2ThO, results from a formal oxidative addition of the OH group of HTh(OH) to the Th(II) center. The formal transfer of the two metal-based electrons from the Th(II) complex to a hydrogen atom leads to the more stable Th(IV) oxidation state in this "thoraformaldehyde" and an increase in the Th−O bond order. The combination of the formation of the new Th−H bond and the increased Th−O bonding leads to the significantly greater stability of H_2ThO relative to HTh(OH). Observation of the latter is likely the result of a kinetic barrier to the rearrangement required for the oxidative addition process.

In the same way that HTh(OH) favors a nonintuitive bent geometry, H_2ThO adopts a nonplanar pyramidal C_s structure in which the Th−O vector is at a 72.4° angle from the H−Th−H plane. To understand the electronic structure of H_2ThO and the source of its nonplanar geometry, we present an MO diagram for planar H_2ThO in Figure 7. We have constructed the MOs using a fragment approach in which two H^- ions interact with a Th(IV) $[ThO]^{2+}$ fragment. Only the 7s and 6d orbitals of Th are included in this description; the Th 5f orbitals are not involved much in the relevant MOs of H_2ThO.

The frontier MOs of $[ThO]^{2+}$, constructed from the O 2s and 2p and Th 7s and 6d atomic orbitals, are shown in the second column from the left of Figure 7. As would be expected from the electronegativity difference between Th and O, the four filled MOs of $[ThO]^{2+}$ are strongly localized on the O atom. The interaction of the 1s AOs of two H^- ions to form planar H_2ThO is shown in the third column from the left of Figure 7. Although the H 1s orbitals can interact in a bonding fashion with the empty Th-localized MOs of $[ThO]^{2+}$, the filled−filled interactions between the filled 1s AOs of H^- and the filled MOs of $[ThO]^{2+}$ dominate. As a consequence, the highest occupied $2b_1$ and $3a_1$ MOs of planar H_2ThO are destabilized relative to the H 1s orbitals. Because of this destabilization and the relatively low-lying vacant Th-based orbitals, the HOMO−LUMO separation in planar H_2ThO is only 2.3 eV.

The electronic structure of planar H_2ThO provides a ready explanation as to why H_2ThO prefers a pyramidal structure.

First, the high-lying HOMO facilitates a pseudo-Jahn−Teller distortion; the distortion of the molecule corresponds to a B_2 vibrational mode, which would couple the $2b_1$ HOMO with the $1a_2$ second lowest unoccupied MO (the separation of the $2b_1$ and $1a_2$ MOs in planar H_2ThO is 3.02 eV). The HOMO is stabilized by this distortion because it allows a significant increase in the contribution of the Th 6d orbitals to the HOMO. Whereas the HOMO of planar H_2ThO contains only 10.7% Th 6d character, the HOMO of pyramidal H_2ThO has 30.9% Th 6d contribution. These highest MOs are stabilized enough by the distortion that the HOMO−LUMO gap is increased to 3.18 eV in pyramidal H_2ThO.

The specific orbital interaction that stabilizes the pyramidal form of H_2ThO is reminiscent of the one that stabilizes bent HTh(OH). In particular, the pyramidal geometry allows an interaction between the antisymmetric combination of the H 1s AOs and the Th 6d AO that has a_2 symmetry in planar H_2ThO (and therefore cannot interact with the H 1s orbitals in the planar geometry):

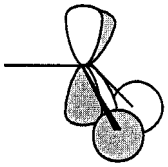

We can make two notable additional observations about this stabilizing interaction: (1) Because there is no analogous low-lying orbital on a C atom, a planar-to-pyramidal distortion is not favored for formaldehyde (H_2CO), and (2) other systems with low-lying empty d orbitals should be subject to the same driving force for a pyramidal distortion. Consistent with this notion, Zhou et al. have predicted that the d^0 complexes H_2MO (M = Ti, Zr, Hf) also exhibit pyramidal structures.[17]

The electronic structure calculations indicate that the unusual bent and pyramidal geometries of the Th complexes reported in this paper are a consequence of increasing the involvement of the Th 6d orbitals in metal−ligand bonding. Inasmuch as the Th 5f orbitals are relatively inaccessible, the Th atom is acting more like a transition metal than an actinide. The ideas advanced in this section are expected to be easily transferable to early transition metal systems with the proviso that the relative energies of the *n*d and (*n* + 1)s orbitals vary from element to element.

V. Reaction Mechanisms

The proposed mechanism of formation of primary reaction products is given below with energies of reactions calculated by relativistic DFT methods (estimated errors ±5 kcal/mol).

$$Th + H_2O \rightarrow [HTh(OH)]^* \rightarrow HTh(OH) \quad (\Delta E = -101 \text{ kcal/mol}) \quad (1)$$

$$Th + H_2O \rightarrow [HTh(OH)]^* \rightarrow H_2ThO \quad (\Delta E = -133 \text{ kcal/mol}) \quad (2)$$

$$Th + H_2O \rightarrow [HTh(OH)]^* \rightarrow H + HThO \quad (\Delta E = -66 \text{ kcal/mol}) \quad (3)$$

$$Th + H_2O \rightarrow 2H + ThO \quad (\Delta E = -4 \text{ kcal/mol}) \quad (4)$$

$$Th + H_2O \rightarrow H + ThOH \quad (\Delta E = -29 \text{ kcal/mol}) \quad (5)$$

$$HThO + H \rightarrow H_2ThO \quad (\Delta E = -67 \text{ kcal/mol}) \quad (6)$$

The initial reaction between energetic[39] laser-ablated thorium atoms and H_2O proceeds through reaction 1 to form the intermediate [HTh(OH)]*. The highly excited [HTh(OH)]* species may relax by collision with the matrix gas to form the matrix-isolated HTh(OH) molecule. However, the main pathways for rearrangement of [HTh(OH)]* are through channels 2 and 3, either by rearranging to the more stable H_2ThO isomer or by breaking the remaining O−H bond. Reaction 5 is another possible way to decompose [HTh(OH)]*. However, it is less favorable as compared to reaction 3; there is no experimental evidence for isolated ThOH. The fact that HThO absorptions do not increase during annealing and irradiation suggests that reaction 2 is too fast to allow elimination of the H-atom, reaction 3, in the matrix. Both reactions 2 and 6 can produce H_2ThO. We believe that reaction 6 is not the mechanism in this experiment, since our Th + H_2/O_2 experiment produced very little H_2ThO. With Th and H_2O, the H_2ThO bands increased markedly upon annealing, which suggests that reaction 2 involves intermediate [HTh(OH)]*, followed by a quick rearrangement and relaxation by the matrix.

In the laser-ablation process, energetic Th atoms can form ThO after elimination of two H atoms, reaction 4, and further reaction can form the more stable tetravalent ThO_2 molecule. Both ThO and ThO_2 will react with H_2O to form secondary products, HThO(OH), $OTh(OH)_2$, for which dramatic increases were observed on annealing to allow reagent diffusion:

$$ThO + H_2O \rightarrow HThO(OH) \quad (\Delta E = -67 \text{ kcal/mol}) \quad (7)$$

$$ThO_2 + H_2O \rightarrow OTh(OH)_2 \quad (\Delta E = -56 \text{ kcal/mol}) \quad (8)$$

In reaction 7, the Th atom in ThO inserts into one O−H bond in H_2O to form a more stable tetravalent molecule HThO(OH). This reaction is confirmed by the concurrent decrease of ThO and increase of HThO(OH) bands on annealing. Reaction 8 may involve a four-member-ring transition state in which one Th═O bond in ThO_2 interacts with one O−H bond in H_2O. The electropositive Th atom forms a new bond with electronegative O atom in H_2O, while the oxygen in Th═O bonds with the H atom in H_2O. As a result, two OH groups will replace the previous Th═O bond in ThO_2 to form $OTh(OH)_2$. A similar four-member-ring transition state has been reported recently in a theoretical study of the TiO_2 reaction with water.[40] The TiO_2 first forms a $TiO_2 \cdot H_2O$ complex, then this intermediate gives a four-member-ring transition state with a barrier of only 5.0 kcal/mol to form finally the oxyhydroxide $OTi(OH)_2$ molecule. The total exothermicity of the reaction of TiO_2 + H_2O to form $OTi(OH)_2$ is 71.2 kcal/mol. Similar behavior is expected for Th atoms since both titanium and thorium have four valence electrons and, as noted earlier, Th should exhibit transition-element-like behavior.

The HThO(OH) molecule formed in the reaction 7 can react with another molecule of H_2O to form $HTh(OH)_3$ via the same four-member-ring transition state:

(39) Kang, H.; Beauchamp, J. L. *J. Phys. Chem.* **1985**, *89*, 3364.
(40) Johnson, J. R. T.; Panas, I. *Inorg. Chem.* **2000**, *39*, 3181.

Scheme 1

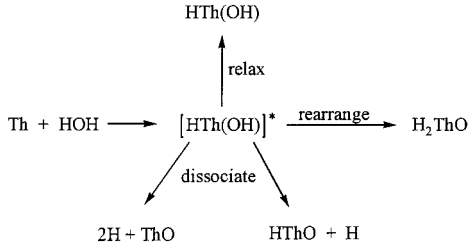

$$HThO(OH) + H_2O \rightarrow HTh(OH)_3 \quad (\Delta E = -59 \text{ kcal/mol}) \quad (9)$$

Because $HTh(OH)_3$ is the product of ThO reacting with two H_2O molecules successively, $HTh(OH)_3$ absorptions increased on 40 K annealing, while all other absorptions decreased.

The reaction between $OTh(OH)_2$ and H_2O could produce $Th(OH)_4$ via a similar four-member-ring transition state. We performed calculations on this molecule with T_d symmetry, and found this closed-shell molecule has a large HOMO−LUMO energy gap, more than 5 eV. Vibrational analyses predicted three strong t_2 modes at 447, 571, and 3849 cm^{-1} with absorption intensities of 404, 173, and 163 km/mol, respectively. Although this molecule appears to be very stable, we see no evidence for it in our experiments, probably because our matrix reactions are not this extensive.

VI. Conclusions

Laser-ablated Th atoms react with H_2O during condensation in excess argon. Although the reaction probably proceeds through insertion to form [HTh(OH)]*, the major products, the rearranged H_2ThO isomer and HThO, are derived from this intermediate as summarized in Scheme 1. Thorium monoxide (ThO) produced in the reaction also inserts into H_2O to produce HThO(OH). Both HThO(OH) and ThO_2 undergo reactions with H_2O to form $HTh(OH)_3$ and $OTh(OH)_2$. Relativistic DFT and ab initio MP2 calculations were performed on all proposed molecules and other possible isomers. Good agreement between experimental and calculated vibrational frequencies, relative absorption intensities, and isotopic shifts has been reached, and the calculated normal-mode frequencies support the infrared absorption assignments. Evidence for divalent and trivalent thorium is found in the ThO and HThO products, and tetravalent thorium in H_2ThO, HThO(OH), and $HTh(OH)_3$. Finally, the new molecules reported here may be initial steps in the important solvation process, and further investigation of the relationship between these Th, H, O species and the Th−H_2O species formed in solution is an interesting topic.

Acknowledgment. The authors gratefully acknowledge financial support from the National Science Foundation (Grant CHE 00-78836 to L.A. and Grant CHE 00-89147 for the Ohio State University Environmental Molecular Sciences Institute) and from the Division of Chemical Sciences, U.S. Department of Energy (Grant DE-FG02-01ER1S135 to B.E.B.), and the Ohio Supercomputer Center and the William R. Wiley Environmental Molecular Sciences Laboratory at Pacific Northwest National Laboratory for grants of computer time.

JA012593Z